X-ray Diffuse Scattering from Wurtzite-Type Compounds

By Kichiro Koto† and Heinz Schulz

Max-Planck-Institut für Festkörperforschung, Heisenbergstrasse 1, 7000 *Stuttgart* 80,
Federal Republic of Germany

Abstract

The diffuse scattering of the wurtzite-type compounds β-AgI, CdS, CdSe, AlN, SiC, ZnO and ZnS has been investigated by X-ray diffraction using film methods. β-AgI, CdS and CdSe show strong non-radial diffuse streak patterns at room temperature, whereas the remaining compounds show only weak or no diffuse scattering. The pattern of the diffuse scattering consists of planes and rods running through the Bragg reflections of the reciprocal lattice of the wurtzite-type compounds. None of these planes and rods runs through the origin of the reciprocal lattice. Most of the diffuse intensity is concentrated in planes parallel to $\{10\bar{1}0\}^*$ and in the rods parallel to a^* and c^* axes. High- and low-temperature experiments indicate a thermal origin of the diffuse scattering. The observed patterns can be explained by the uncorrelated thermal vibrations of structural units as chains and layers. The intensity shows a correlation to the ionicity and bond length of the investigated wurtzite-type compounds.

Introduction

The non-radial diffuse streak patterns in many crystals are caused by the thermal motion of the atoms. It can be explained by acoustical and optical modes of lattice vibrations with low frequencies (Komatsu & Teramoto, 1966). This holds, for example, for diffuse scattering of hexagonal ice (Owston, 1949). In the structure of hexagonal ice, the arrangement of the oxygen atoms is approximately the same as in the wurtzite-type compounds, without taking hydrogen atoms into consideration. From this structural point of view, a diffuse streak pattern similar to ice is expected for wurtzite-type compounds. This has been confirmed by our experimental results.

In the study of the lattice dynamics of wurtzite-type CdS (Nusimovici, Balkanski & Birman, 1970), optical modes with low frequencies have been found in the direction along Σ and Δ, which lead to diffuse scattering. Bührer & Brüesch (1975) have investigated

the phonon dispersion of single crystals of β-AgI by inelastic neutron scattering. In addition to the acoustic modes, they observed a low-lying optical mode at 2 meV with a flat dispersion along Σ and Δ. Beyeler, Brüesch, Hibma & Bührer (1978) have observed the X-ray diffuse scattering from β-AgI single crystals independently from the present authors (Koto & Schulz, 1978). They calculated the expected diffuse streak patterns using a lattice dynamical model.

Experimental

The wurtzite-type compounds AlN, β-AgI, CdS, CdSe, SiC, ZnO and ZnS were studied. Synthetic materials, except for zincite ZnO (Franklin Furnace, New Jersey, USA), were used in the experiments. The crystals had cross sections of 1–4 mm² and thicknesses of $0 \cdot 1$–$0 \cdot 5$ mm. The X-ray beam had a diameter of $0 \cdot 5$ mm. Precession and fixed crystal–fixed film photographs were taken with Mo $K\alpha$ radiation (45 kV and 35 mA) monochromatized by pyrolytic graphite.

The crystals were exposed to X-rays *in maximus* for five days. The photographs were taken in different crystallographic directions. Temperature dependence of the diffuse scattering was also investigated by the fixed crystal–fixed film technique for the compounds of β-AgI, ZnO and ZnS at various temperatures. The high-temperature experiment was done by heating the crystals in an air stream. The low-temperature photographs were taken with the crystals cooled in a nitrogen stream. Heating and cooling were carried out with an accuracy of ± 5 K.

β-AgI, CdS and CdSe single crystals show strong non-radial diffuse streak patterns at room temperature (Figs. 1, 2, 3 and 4). Photographs of β-AgI were also taken in the temperature range from 120 to 400 K. The features of the diffuse scattering remained unchanged in this temperature range. However, comparison of the photographs at different temperatures indicated that the diffuse-scattering intensity became weaker with decreasing temperature, but the diffuse streak pattern was still observed at 120 K. AlN and ZnS showed similar, but very weak diffuse streak patterns at room temperature and 670 K, respectively. No diffuse streak

---

pattern was observed from SiC and ZnS at room temperature and from ZnO at room temperature and 770 K. The results are listed in Table 1.

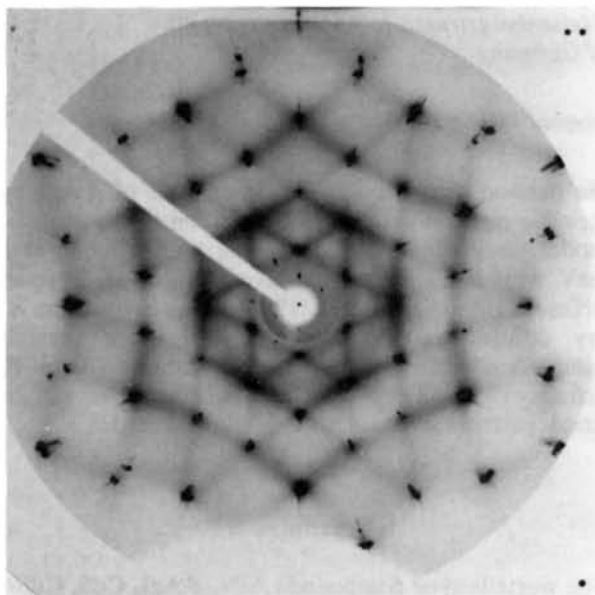The main features of the diffuse scattering from the wurtzite-type compounds are as follows. The intensity of non-radial diffuse streak patterns is mostly concentrated in the reciprocal planes parallel to $\{10\bar{1}0\}^*$. These diffuse-scattering planes run through the Bragg reflections of the fundamental wurtzite structure. However, no diffuse planes run through the origin of the reciprocal space. In addition, weak diffuse intensity was observed in the planes parallel to $\{10\bar{1}1\}^*$. In the

Fig. 1. Diffuse scattering from β-AgI at room temperature taken by the fixed crystal–fixed film technique. Monochromatized Mo $K\alpha$ radiation along the c axis. The diffuse scattering pattern comes from the intersection of the Ewald sphere and diffuse scattering planes parallel to $\{10\bar{1}0\}^*$ in reciprocal space.
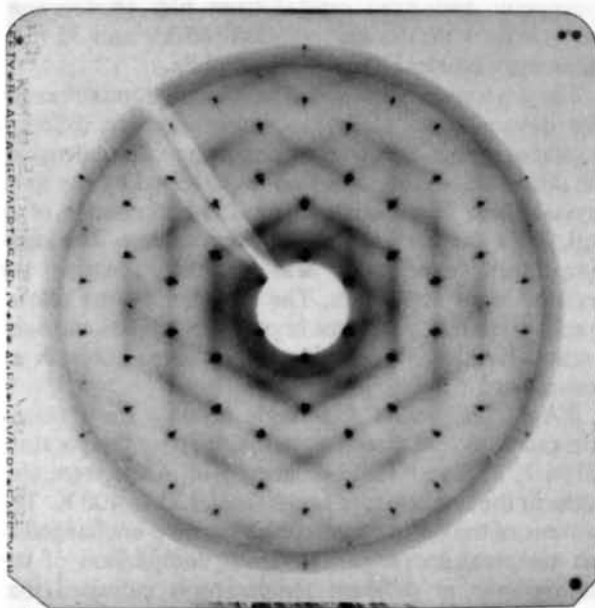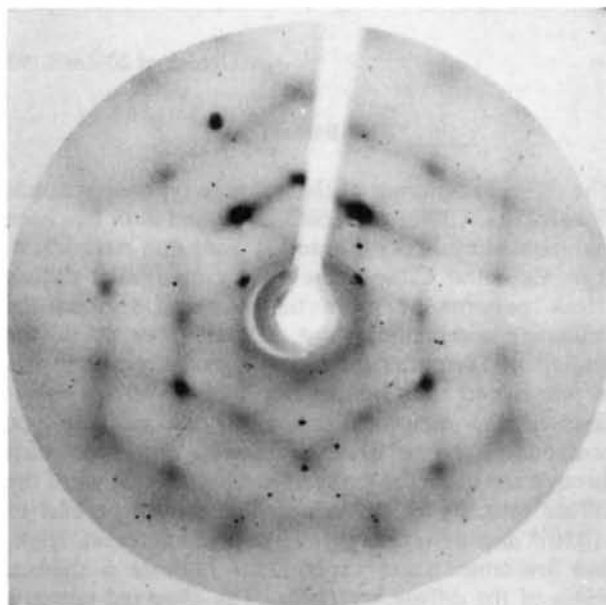

Fig. 3. Fixed crystal–fixed film photograph of CdS at room temperature. X-rays 10° from the c axis. A similar diffuse streak pattern to that from β-AgI (Fig. 1) is observed.
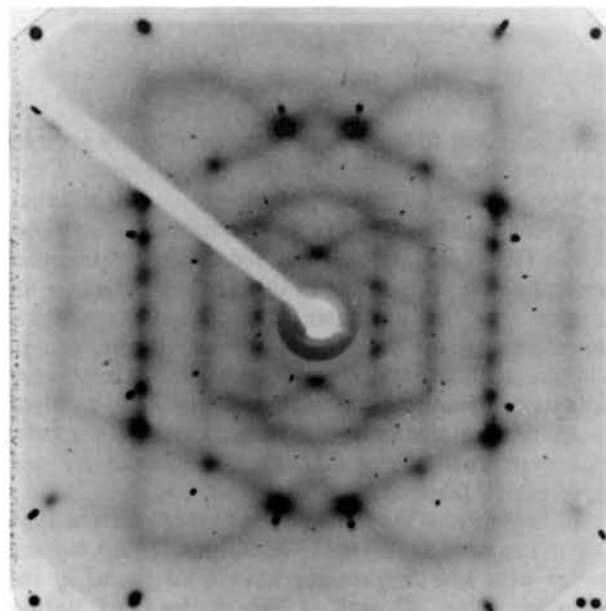

Fig. 2. First level of precession photograph parallel to $(0001)^*$ from β-AgI at room temperature. Diffuse streak pattern is along the a^* axes through the Bragg reflections and the positions of systematic absences (e.g. $11\bar{2}1$, $22\bar{4}1$). No diffuse streaks are observed through the origin of the first level of $(0001)^*$.

Fig. 4. Fixed crystal–fixed film photograph of CdS at room temperature. X-rays parallel to the a axis. Diffuse streak pattern due to the diffuse scattering planes parallel to $\{10\bar{1}1\}^*$ is observable in addition to those parallel to $\{10\bar{1}0\}^*$.

diffuse-scattering planes parallel to $\{10\bar{1}0\}^*$, strong intensity is observed on rods, which run through the Bragg reflections and are parallel to the a^* and c^* axes. It follows that diffuse scattering intensity can be observed at the forbidden Bragg reflections such as $11\bar{2}1$, $22\bar{4}1$, etc. of the space group $P6_3mc$ for wurtzite-type compounds. The intensity distributions of β-AgI, CdS, CdSe, AlN and ZnS are approximately the same in spite of the different constituent atoms.

Results and discussion

The temperature dependence of the observed diffuse scattering intensity indicates its thermal origin. The intensity is correlated to the ionic character and the bond distances of the wurtzite-type compounds as shown in Table 1. With decreasing ionicity and bond length, diffuse scattering intensity decreases when going from β-AgI to SiC.

The main features of the diffuse scattering patterns are explained by dividing the wurtzite-type structure (Fig. 5a) into structural units of layers and chains (Fig. 5b–e). Bonds among these units are exactly or approximately perpendicular to each other. In crystals with ionic character, bond bending modes have vibrations of low energies. Such vibrations can be excited if the direction of the distortion is perpendicular to the bonds. We assume correlated thermal motion of the atoms within the above mentioned structural units and uncorrelated thermal motion of these units to each other. This gives rise to nearly dispersionless, low-energy phonon branches as described below. The corresponding superimposed diffuse scattering generates just the main features of the observed scattering patterns.

In the following, the proposed structural units, the diffuse scattering generated by their uncorrelated thermal motions and the phonons corresponding to the thermal motions of these structural units are described.

(1) Zigzag chains run parallel to the a axis (Fig. 5b). Bonds between these chains are exactly perpendicular to the chains. Their thermal motion generates the

diffuse layers parallel to $\{10\bar{1}0\}^*$. Actually, most of the diffuse intensity is concentrated in these reciprocal planes. This can be described by transversal branches with wave vectors $\mathbf{q}$ perpendicular to the a axis and with polarization vectors $U(\mathbf{q})$ parallel to the a axis.
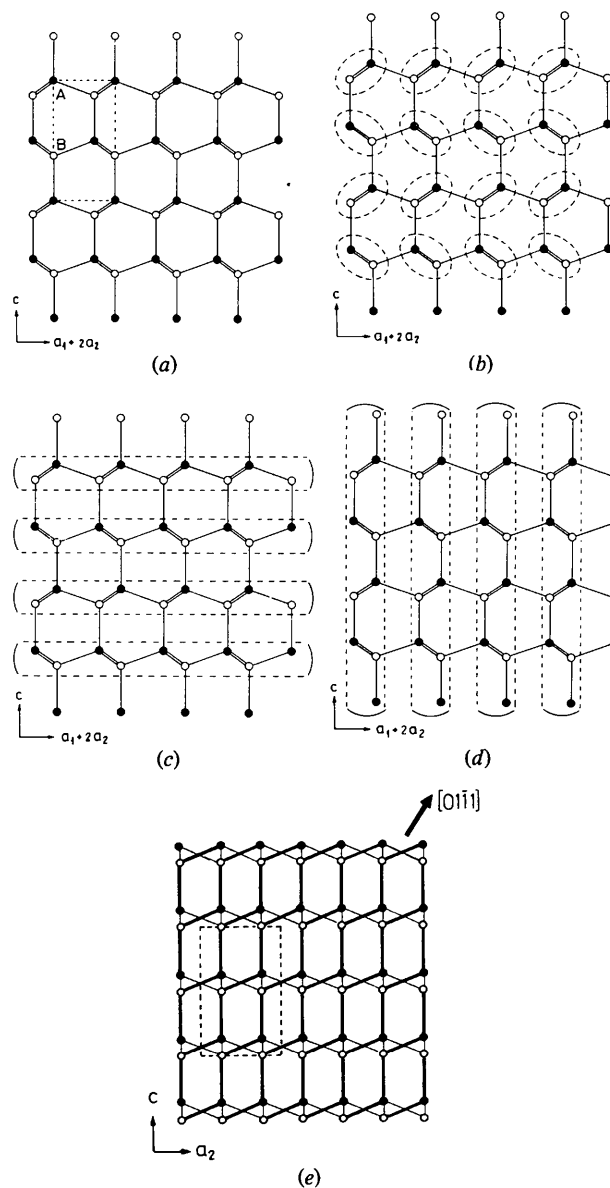

Fig. 5. Structural units in the form of chains and layers. The units are perpendicular to the plane of the drawing in (b), (c) and (d), and parallel to the plane of the drawing in (e). Solid and open circles represent cations and anions in the wurtzite-type structure. (a) Projection of the wurtzite structure along the a axis. The unit cell is indicated by the dotted line. (b) Structural units of zigzag chains of A–B–A–B– atoms. (c) Structural units in the form of layers parallel to (0001). (d) Structural units in the form of layers parallel to ($10\bar{1}0$). (e) Projection perpendicular to ($10\bar{1}0$). The unit cell is indicated by the dotted line. Structural units of chains parallel to [$01\bar{1}1$] are shown by the thick line. The bonds between the chains are indicated by the thin lines.

Table 1. *Investigated wurtzite-type compounds*

Compound	Intensity of the diffuse scattering	Investigation temperature	Ionicity f_i	Bond distance (Å)
β-AgI	strong	120–400 K	0·770	2·80
CdSe	strong	room temperature	0·699	2·62
CdS	strong	room temperature	0·685	2·53
ZnS	weak	670 K	0·623	2·35
ZnO	–	770 K	0·616	1·97
AlN	very weak	room temperature	0·449	1·89
SiC	–	room temperature	0·177	1·89

The ionicity, f_i, is based on the Philips scale and is taken from Van Vechten (1969).

This means that $\mathbf{q}$ lies in the plane of Fig. 5(b) and $U(\mathbf{q})$ is parallel to the zigzag chains.

(2) Structural units in a form of layer exist parallel to (0001) (Fig. 5c). Bonds between these layers are exactly perpendicular to (0001). The strong diffuse streaks parallel to the c^* axis and running through the Bragg reflections in the $\{10\bar{1}0\}^*$ can be explained by their thermal motion. This corresponds to transversal branches with $\mathbf{q}$ parallel to the c axis and $U(\mathbf{q})$ perpendicular to the c axis.

(3) Structural units in a form of layer exist parallel to $\{10\bar{1}0\}$ (Fig. 5d). Bonds between these layers are nearly perpendicular to $\{10\bar{1}0\}$. The strong diffuse streaks parallel to the a^* axis and running through the Bragg reflections in the $\{10\bar{1}0\}^*$ can be explained by transversal branches with $\mathbf{q}$ parallel to the a^* axis and $U(\mathbf{q})$ perpendicular to the a^* axis. a_1^* is parallel to $a_1 + 2a_2$ as shown in Fig. 5(d).

(4) Structural units in a form of chains exist parallel to $\langle 10\bar{1}1 \rangle$ (Fig. 5e). The diffuse layers parallel to $\{10\bar{1}1\}^*$ are explained also by transversal branches with $\mathbf{q}$ perpendicular to $\langle 10\bar{1}1 \rangle$ and with polarization vectors $U(\mathbf{q})$ parallel to $\langle 10\bar{1}1 \rangle$.

The main features of the diffuse streak patterns observed with the wurtzite-type compounds are generated by superposition of the different scattering features described under (1) to (4). The intensity scattered by one of the proposed soft modes can be calculated by the structure factor

$$F(\mathbf{s}) = \sum_n \frac{f_n \sqrt{E(\mathbf{q})}}{\sqrt{m_n \, v(\mathbf{q})}} [\exp 2\pi i (\mathbf{s} . \mathbf{r}_n)][\mathbf{s} . U(\mathbf{q})], \quad (1)$$

$$\mathbf{s} + \mathbf{q} = \mathbf{H}. \quad (2)$$

Here, f_n, m_n and r_n are the atomic scattering factor, atomic mass and position vector of the nth atom in a unit cell. $E(\mathbf{q})$, $v(\mathbf{q})$ and $U(\mathbf{q})$ are respectively the mean phonon energy, the frequency and the polarization vector belonging to the wave vector $\mathbf{q}$. $\mathbf{H}$ is the reciprocal lattice point nearest to $\mathbf{s}$. In order to get an estimate of the scattered intensity in the wurtzite-type compounds, we make the following simplifications (this means just 'uncorrelated thermal motion of structural elements'):

$$F(\mathbf{s}) \propto \sum_n \{\exp 2\pi i (\mathbf{s} . \mathbf{r}_n)\}\{\mathbf{s} . U(\mathbf{q})\}. \quad (3)$$

The first term in the sum of (3) is the usual structure factor of the atomic arrangement. For $l \simeq 0$ it gives the following intensity modulation

$$I(\mathbf{s}) \propto 4 \cos^2 [\pi (h - k)/3]. \quad (4)$$

Equation (4) is calculated by replacing $\mathbf{s}$ and $\mathbf{r}_n$ by the usual component description. It describes roughly the intensity variation along the rods in Fig. 1. The intensity distribution according to (4) is modified by the term $\{\mathbf{s} . U(\mathbf{q})\}$ of (3). It describes the contribution of the phonons to the observed intensities. Neglecting phase differences for phonons near the edge of the Brillouin zone, the contributions of the term are in phase for the described acoustical phonons but in anti-phase for the optical phonons. Owing to the antiphase vibrations, intensity can be observed at reflections not allowed by the space-group symmetry. The second part of (3) is also responsible for the absence of streaks running through the origin of the reciprocal space. For these streaks $\mathbf{s} . U(\mathbf{q}) = 0$.

Table 1 shows a jump in the diffuse intensity observed in our experiments. The silver and cadmium compounds generate strong diffuse scattering, all other compounds show only weak or no diffuse scattering. The observation of the weak diffuse intensity depends on experimental conditions, $e.g.$ crystal shape and size, absorption of X-rays, secondary X-rays and so on. There exist correlations with the ionicity of the compounds and also with their bond distances. However, these quantities vary smoothly and do not show a jump, which correlates with the diffuse scattering of the wurtzite-type compounds listed in Table 1. Therefore, we conclude that the features of the diffuse scattering described in this paper are present in all wurtzite-type compounds. The intensities depend on the relation between investigation temperature and melting or transition temperature and on the electrons involved in the bonding. Only the silver and cadmium atoms use 5s and 5p electrons for generating the bonds. Our experiments suggest that bonds formed with these electrons can easily be distorted.

References

Beyeler, H. U., Brüesch, P., Hibma, T. & Bührer, W. (1978). *Phys. Rev. B*, **18**, 4570–4575.

Bührer, W. & Brüesch, P. (1975). *Solid State Commun.* **16**, 155–158.

Komatsu, K. & Teramoto, K. (1966). *J. Phys. Soc. Jpn*, **21**, 1152–1159.

Koto, K. & Schulz, H. (1978). *Acta Cryst.* A**34**, S289.

Nusimovici, M. A., Balkanski, M. & Birman, J. L. (1970). *Phys. Rev. B*, **1**, 595–603.

Owston, P. G. (1949). *Acta Cryst.* **2**, 222–228.

Van Vechten, J. A. (1969). *Phys. Rev.* **187**, 1007–1020.